Magnetic Resonance in Medicine 68:762–771 (2012)

Simultaneous Measurement of Cerebral Blood Flow and Transit Time with Turbo Dynamic Arterial Spin Labeling (Turbo-DASL): Application to Functional Studies

Yuguang Meng,* Ping Wang, and Seong-Gi Kim

A turbo dynamic arterial spin labeling method (Turbo-DASL) was developed to simultaneously measure cerebral blood flow (CBF) and blood transit time with high temporal resolution. With Turbo-DASL, images were repeatedly acquired with a spiral readout after small-angle excitations during pseudo-continuous arterial spin labeling and control periods. Turbo-DASL experiments at 9.4 T without and with diffusion gradients were performed on rats anesthetized with isoflurane or α-chloralose. We determined blood transit times from carotid arteries to cortical arterial vessels (TT_a) from data obtained without diffusion gradients and to capillaries (TT_c) from data obtained with diffusion gradients. Cerebral arterial blood volume (CBV_a) was also calculated. At the baseline condition, both CBF and CBV_a in the somatosensory cortical area were 40–50% less in rats with α-chloralose than in rats with isoflurane, while TT_a and TT_c were similar for both anesthetics. Absolute CBF and CBV_a were positively correlated, while CBF and TT_c were slightly negatively correlated. During forepaw stimulation, CBF increase was 15 ± 3% (n = 7) vs. 60 ± 7% (n = 5), and CBV_a increase was 19 ± 9% vs. 46 ± 17% under isoflurane vs. α-chloralose anesthesia, respectively; CBF vs. CBV_a changes were highly correlated. However, TT_a and TT_c were not significantly changed during stimulation. Our results support that arterial CBV increase plays a major role in functional CBF changes. Magn Reson Med 68:762–771, 2012. © **2011 Wiley Periodicals, Inc.**

Key words: cerebral blood flow; transit time; arterial cerebral blood volume; forepaw stimulation

Arterial spin labeling (ASL) MRI (1–4) can be used to quantify in vivo tissue perfusion, such as cerebral blood flow (CBF), without using a contrast agent. With this technique, water proton nuclear spins in arterial blood are magnetically labeled and used as freely diffusible tracers to observe perfusion rates with MRI. ASL can be achieved either by continuous ASL, in which a long radio frequency (RF) pulse, on the order of seconds, inverts the proton magnetization in the carotid arteries (1) or by pulsed ASL in which a relatively short RF pulse, on the order of milliseconds, changes the longitudinal magnetization of the arterial blood in a slab proximal to the imaging section of interest (2–4). Following spin labeling, arterial blood travels from the labeling plane to capillaries where it exchanges with tissue water, resulting in a change in tissue proton magnetization. The arterial blood transit time (TT) from the labeling plane to the vascular compartment within an imaging pixel is an important parameter for determining CBF (5) and may be sensitive to vascular viability and related to disease pathology (6,7). Thus, it is crucial to measure the arterial blood TT in normal and pathological subjects.

With pulsed ASL measurements, repeated acquisitions of ASL images with small flip angle excitations can be performed after the ASL pulse (8–12), allowing the rapid detection of multiple spin labeling time points. These methods include Look-Locker flow-sensitive alternating inversion-recovery (8), inflow turbo-sampling flow-sensitive alternating inversion-recovery (9), turbo transfer insensitive labeling (10), and rapid acquisitions after signal targeting with alternating RF ASL (11,12). With dynamic ASL (DASL) models (8–12), arterial blood TT and CBF have been successfully determined in humans; however, low sensitivity limits its application in rodent models. With continuous ASL measurements, TTs can be determined by varying the postlabeling delay (7,13,14) or by using the dynamic ASL (DASL) technique (15,16). With DASL, images are acquired during repeated on-and-off periods of a long ASL pulse (i.e., three times longer than T_1 of tissue). To improve temporal resolution of ASL signals, the onset time of each ASL pulse is shifted relative to MRI data collection. DASL has been used to simultaneously measure arterial blood TT and CBF in rats (15,16) but the long experimental time limits its utility for dynamic studies, such as functional MRI (fMRI).

Arteries and arterioles that supply blood to capillaries near active neurons actively dilate during functional stimulation (17,18). If we model blood flow according to the Poiseuille's equation describing the relationship between flow, resistance, and pressure of a Newtonian fluid in a long straight tube, a 10% increase of vessel diameter (i.e., 21% cerebral blood volume [CBV] increase) should induce a 46% increase in blood flow. This relationship also suggests that increased arterial CBV (CBV_a) will also result in shorter arterial blood TTs. This expectation appears to be supported by human fMRI measurements (8,10,12,14,19), where increases in functional CBF are accompanied by shorter TTs. However, in our previous functional measurements during somatosensory stimulation in isoflurane-anesthetized rats (20), relative changes in CBF and CBV_a were similar, suggesting that there was no significant change in the arterial

Neuroimaging Laboratory, Department of Radiology, University of Pittsburgh, Pittsburgh, Pennsylvania, USA.

Grant sponsor: National Institutes of Health; Grant numbers: EB003324, EB003375, NS44589.

*Correspondence to: Yuguang Meng, Ph.D., Department of Radiology, School of Medicine, University of Pittsburgh, 3025 E. Carson Street, Pittsburgh, PA 15203. E-mail: mengyg@gmail.com

Received 1 February 2011; revised 21 September 2011; accepted 17 October 2011.

DOI 10.1002/mrm.23294

Published online 9 December 2011 in Wiley Online Library (wileyonlinelibrary.com).

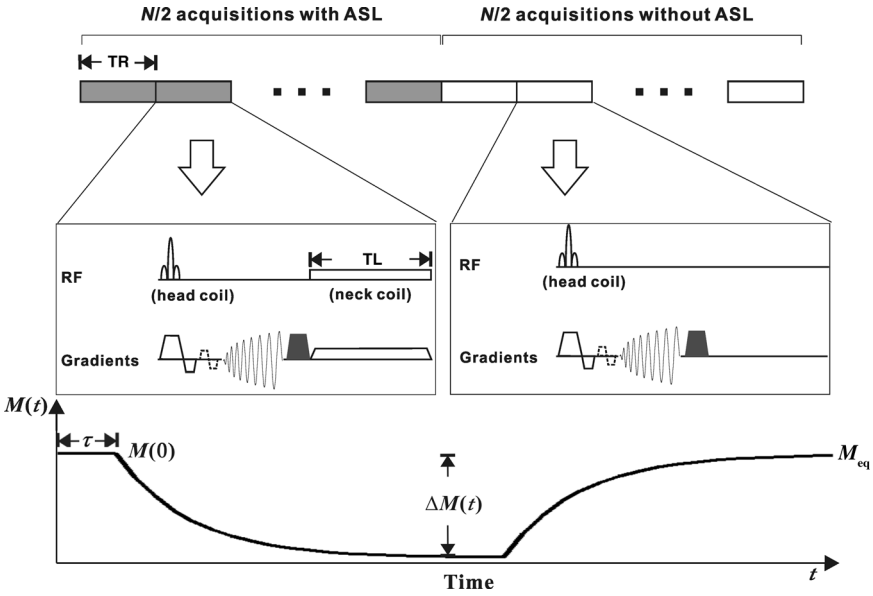

FIG. 1. Schematic diagrams of the Turbo-DASL pulse sequence (top) and the expected signal response (bottom). A cycle of *N* images with TR consists of *N*/2 acquisitions with ASL and the other *N*/2 without ASL. Spiral data collection is applied after a low flip angle excitation RF pulse for obtaining short TE images and followed by a magnetization-dephasing gradient pulse (filled trapezoid). Diffusion gradients (dashed trapezoids) are optionally applied to eliminate arterial blood signal and to measure blood TT to capillaries. Arterial spin labeling pulse with TL is applied using a neck labeling coil along with *z*-axis gradient around the carotid arteries. The signal $M(t)$ varies with respect to time t. τ is the cerebral blood TT from the carotid arteries to vasculature in the imaging slice, and $M(0)$ and M_{eq} are the signal intensities at $t = 0$ and steady state in the presence of repetitive excitations, respectively. $\Delta M(t)$ is the signal difference between labeling and control periods with respect to time t.

blood TT. Thus, direct measurement of arterial blood TTs with high temporal resolution is necessary to determine if stimulation leads to changes in arterial blood TTs in rodent models, and if our previous observation resulted from the use of isoflurane.

In this work, a modified DASL method was implemented with rapid repetition of data collection during pseudocontinuous ASL and control periods, which we refer to as Turbo-DASL. Turbo-DASL experiments at 9.4 T with a temporal resolution of 4 s were performed on isoflurane- and α-chloralose-anesthetized rats during forepaw stimulation. Studies have shown that isoflurane increases the baseline CBF and blunts the evoked CBF response, while α-chloralose has a lower baseline CBF and exhibits a higher CBF response (20,21). To measure blood TTs from carotid arteries to cortical arterial vessels (TT_a) and to capillaries (TT_c), Turbo-DASL was performed without and with flow-crushing bipolar diffusion gradients. CBV_a was also calculated from ASL signals acquired with and without diffusion gradients (22). Baseline and evoked CBF, TT_a, TT_c, and CBV_a in the somatosensory cortex were measured and compared in rats under isoflurane or α-chloralose anesthesia.

THEORY

The Turbo-DASL technique was implemented with rapid repetition of spiral data acquisition for improved temporal resolution. Figure 1 shows the schematics of the imaging protocol, pulse sequence, and expected MRI signal. In one Turbo-DASL cycle consisting of N images with a repetition time (TR), the first half of the images are acquired with ASL, and the second half of the images are acquired without ASL as a control. A spin labeling pulse with duration labeling time (TL) is applied between each spiral image acquisition and subsequent excitation pulse. To minimize the magnetization transfer effect in imaging slices, actively decoupled neck and head coils can be used for spin labeling and for data acquisition, respectively. The time-dependent magnetization during one Turbo-DASL cycle is dependent on perfusion and the apparent longitudinal relaxation rate (R_{1app}) in the presence of repeated excitations (see Fig. 1 expected time course). $R_{1app} = R_1 - \ln(\cos\theta)/TR$ where R_1 is the spin-lattice relaxation rate of tissue water and θ is the flip angle of the excitation pulses (9). The magnetization at time t, $M(t)$ is described as

$$M(t) = M(0)e^{-t\cdot R'_{1app}} + M_{eq}(1 - e^{-t\cdot R'_{1app}}) - \Delta M(t), \quad [1]$$

where $M(0)$ is the magnetization at $t = 0$; M_{eq} is the magnetization at the steady-state condition; $\Delta M(t)$ is the perfusion-induced magnetization due to ASL; and $R'_{1app} = R_{1\ app} + f / \lambda$ where f is the CBF and λ is the brain-to-blood partition coefficient. $\Delta M(t)$ can be solved using the general kinetic model proposed by Buxton et al. (23), in which blood tracer (spin) delivery function $c(t)$ is convolved with tracer decay (i.e., magnetization relaxation) $m(t)$ and residual function $r(t)$.

When t is shorter than the blood TT from the labeling position to the imaging pixel τ, $\Delta M(t)$ is zero and $M(t)$ is constant if $M(0) = M_{eq}$. When the arterial signal contribution is significant, a two-compartment (tissue and artery) model is valid. For simplicity, a one-compartment ASL

model is applied here with the assumption that blood exchanges with extravascular tissue water rapidly. When $t \geq \tau$, $\Delta M(t)$ is

$$\Delta M(t) = \frac{2M_0 f}{\lambda} \int_0^t c(t') \cdot r(t-t') m(t-t') \mathrm{d}t' \qquad [2]$$

where M_0 is the fully relaxed tissue magnetization. The delivery function $c(t) = \alpha_0 e^{-\tau \cdot R_{1a}}$, where α_0 is the degree of spin labeling at the labeling position and R_{1a} is the spin-lattice relaxation rate of arterial blood water. As pseudocontinuous ASL is proposed in Fig. 1, α_0 is (TL/TR) of the spin labeling efficiency measured with continuous ASL, assuming that the labeled spins in arterial vasculature are not perturbed by excitation RF pulses before they exchange with tissue spins. The residual function is $r(t) = e^{-t \cdot f/\lambda}$, and the tracer decay function is $m(t) = e^{-t \cdot R_{1app}}$. Eq. 2 can be rewritten as

$$\Delta M(t) = \begin{cases} 0 & t < \tau \\ \frac{2M_0 \alpha_0 e^{-\tau \cdot R_{1a}} f}{\lambda R'_{1app}} \left[e^{-\max(t-\Delta-\tau, 0) R'_{1app}} - e^{-(t-\tau) \cdot R'_{1app}} \right] & t \geq \tau \end{cases}, \qquad [3]$$

where the *max* function returns the larger of the two values and $\Delta = (N/2)\mathrm{TR}$. During the first set of $N/2$ images, with ASL, the magnetization decays according to $(1 - e^{-(t - \tau) \cdot R'_{1app}})$ at $t > \tau$. During the second set of $N/2$ images, the magnetization begins to recover to M_{eq} at $t > \Delta + \tau$. To obtain CBF (f) and blood TT from the Turbo-DASL data using Eqs. 1 and 3, α_0, M_0, and R'_{1app} need to be determined. The spin labeling efficiency is measured in the usual manner, and M_0 and R'_{1app} can be determined from a fit of signal decay, $M(t)$, obtained with the same imaging parameters, but without ASL. $M(0)$, M_{eq}, f, and τ are then determined from one Turbo-DASL cycle (see Fig. 1). τ is the blood TT from the labeling plane to the cortical arterial vessels (TT_a) in the absence of flow-crushing gradients and to the capillaries (TT_c) when flow-crushing gradients are applied before data acquisition.

MATERIALS AND METHODS

Animal Preparation

This study used 13 male Sprague-Dawley rats weighing 350–450 g (Charles River Laboratories, Wilmington, MA), and all procedures were approved by the University of Pittsburgh Institutional Animal Care and Use Committee. Animals were initially induced with 5% isoflurane in a mixture of medical air and O_2 gases, then intubated and mechanically ventilated. The femoral artery was catheterized for blood sampling and pressure monitoring. During the imaging experiments, animals were maintained with an air:O_2 mixture such that the fraction of inspired oxygen was 30%. Animals were anesthetized with 1.5% isoflurane ($n = 8$) or an infusion of α-chloralose (an initial 55 mg/kg i.v. bolus followed by 25 mg/kg/h; $n = 5$). Blood gases were sampled intermittently. The arterial blood pressure and the breathing pattern were recorded with a multitrace recorder (AcKnowledge, Biopak, CA). End-tidal CO_2, blood gases, and blood pressure were kept within normal physiology ranges, and body temperature was maintained at 37.5°C using a circulating water pad.

Imaging Experiment

All MRI experiments were performed on a 9.4 T, 31-cm-bore MRI system (Varian, Palo Alto, CA), equipped with an actively shielded 12-cm inner diameter gradient insert (Magnex, Abingdon, UK), which operates at a maximum gradient strength of 400 mT/m and a rise time of 120 μs. Two actively decoupled coils were used: a neck coil for ASL and a surface coil for imaging brain. Localized shimming was performed over a volume covering the imaging region to yield a water spectral linewidth of less than 30 Hz. Anatomical T_1-weighted images were acquired with a conventional Turbo Fast Low Angle SHot (TurboFLASH) using an inversion time of 1.4 s. A single 2-mm-thick coronal slice covering the primary somatosensory cortex was selected according to anatomical images, multislice scout fMRI data, and rat brain atlas (24).

All Turbo-DASL images were acquired with a single-shot spiral readout (25). The imaging parameters were as follows: flip angle in the contralateral primary somatosensory cortex = 21–27°, measured by the B_1 mapping method with doubling of the RF power (26); echo time (TE) = 6 ms; matrix size = 64 × 64; field of view = 2.56 × 2.56 cm^2; off-resonance frequency for ASL = 8500 Hz; and z-axis gradient strength for ASL = 1 G/cm. To determine M_0 and R'_{1app}, 20 images were acquired with the same imaging parameters used for Turbo-DASL but without the ASL pulse. To determine whether f and τ are sensitive to experimental parameters, Turbo-DASL experiments (without stimulation) were performed in one isoflurane-anesthetized animal with TR = 100 and 200 ms with TL = 70 and 170 ms, respectively, and $N = 40$ and 80.

For functional studies in seven isoflurane-anesthetized and five α-chloralose-anesthetized animals, Turbo-DASL experiments with $N = 40$ images, TR = 100 ms, and TL = 70 ms were performed without and with flow-crushing diffusion gradients ($b = 50$ s/mm^2), which minimizes arterial blood signals (22). The flow-crushing gradients were simultaneously applied to all three axes to minimize the duration of the gradient pulse and consequently TE. Somatosensory stimulation was performed on one forepaw by repeated electric pulses with the parameters optimized under isoflurane anesthesia (pulse duration: 1 ms, current: 1.3–1.4 mA, and frequency: 6 Hz) (27,28) or under α-chloralose anesthesia (pulse duration: 0.3 ms, current: 2.0 mA, and frequency: 3 Hz) (21). One fMRI run consisted of five baseline (20 s), five stimulation (20 s), and 10 baseline (40 s) cycles, with inter-run delay of > 2 min. About 50 runs were repeated.

Data Processing and Analysis

All image reconstruction and computations were carried out off-line with MATLAB (MathWorks, Natick, MA) scripts. All repeated fMRI runs with the same imaging parameters were combined to obtain one averaged fMRI run for each subject. No image coregistration, spatial

smoothing, or temporal and spatial filtering was conducted. M_0 ($M(0)$ in Eq. 1) and R'_{1app} were determined from 20 images without ASL using Eq. 1 without the $\Delta M(t)$ term. As the degree of spin-labeling in the labeling position, measured with the method as described in (29), was 0.7 with our setup, the labeling efficiency, α_0, was assumed to be 0.7 × (TL/TR). R_{1a} is 0.43 s^{-1} at 9.4 T (30). With these parameters and using a brain-to-blood partition coefficient, λ, of 0.9 g/ml, f, τ, $M(0)$, and M_{eq} were determined for each Turbo-DASL cycle with a pixel-by-pixel or region-by-region fit using Eqs. 1 and 3. Data were recorded as the mean ± SD for statistical analysis.

To determine the effects of imaging parameters TR and N on the fitted parameters (i.e., CBF and TT) of Turbo-DASL, datasets from one animal without stimulation were analyzed. All repeated Turbo-DASL cycles with the same imaging parameters were averaged, resulting in one Turbo-DASL cycle for each experimental condition. Then, somatosensory cortical and large vessel regions of interest (ROIs) were chosen, based on the brain atlas and anatomic images. Time courses from one Turbo-DASL cycle were obtained from these ROIs.

For fMRI data (n = 12), baseline CBF and TT maps were obtained from one averaged prestimulus Turbo-DASL cycle for each animal. Time-dependent CBF and TT maps were also determined on a Turbo-DASL cycle-by-cycle basis, and functional maps were generated using a boxcar cross-correlation method with a cross-correlation threshold of 0.5 and the number of cluster pixels of 3. Then, the percent signal changes were calculated from active pixels.

To compare quantitative CBF and TT values between baseline and stimulation periods, we selected one contralateral somatosensory ROI with 3 × 3 pixels, based on the anatomical T_1-weighted image and stereotaxic coordinates of forelimb area (24). We obtained several pieces of information. First, time courses of CBF and TT were determined from ROI-based Turbo-DASL data. Second, baseline values were calculated from one averaged prestimulus Turbo-DASL cycle. Third, physiological values during stimulation were calculated from one averaged stimulation Turbo-DASL cycle except the transition period 0–4 s after the onset of stimulation. In addition, we calculated CBV_a from the signals acquired with and without diffusion gradients as (22)

$$CBV_a = \lambda \frac{\Delta M(0)/M_0(0) - \Delta M(b)/M_0(b)}{2\alpha_a \cdot \xi - \Delta M(b)/M_0(b)}, \quad [4]$$

where $\Delta M(0)$ and $\Delta M(b)$ are the differences between the first and last (i.e., $N/2$ image) signals during ASL in each Turbo-DASL cycle acquired without and with diffusion gradients, respectively; $M_0(0)$ and $M_0(b)$ are the fully relaxed initial magnetization M_0 values acquired without and with diffusion gradients, respectively; α_a is $\alpha_0 \cdot \exp(-TT_a \cdot R_{1a})$ that is the effective labeling efficiency considering the arterial blood magnetization relaxation during TT_a; and $\xi = \exp[-(R_{2a}^* - R_{2t}^*) \cdot TE]$ in which R_{2a}^* and R_{2t}^* are the apparent transverse relaxation rates (i.e., R_2^*) of arterial blood and tissue, respectively, and ξ is considered to be 1, because of the short TE (i.e., 6 ms) used here (22).

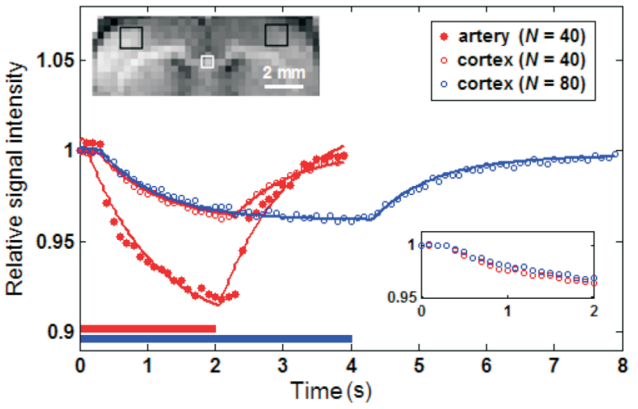

FIG. 2. Regional MR signals during one averaged Turbo-DASL cycle acquired with different imaging parameters without diffusion gradients, from one isoflurane-anesthetized animal. Turbo-DASL data were obtained from somatosensory cortex regions (black boxes in the inset image) and artery-containing ROI (white box) and were fitted with Eq. 1 (see solid lines). The single-compartment model fits very well to the cortical data but not to data containing significant signal from large arteries. Bars underneath Turbo-DASL time courses indicate ASL durations. Inset time courses show 0 to 2 s data points of the somatosensory ROI for better visualization. [Color figure can be viewed in the online issue, which is available at wileyonlinelibrary.com.]

RESULTS

Baseline Turbo-DASL Without Stimulation

Figure 2 shows the time-dependent Turbo-DASL signal from a single isoflurane-anesthetized rat with different imaging parameters. Data are shown from tissue ROIs in the somatosensory cortex and an artery-containing ROI. Signals exponentially decreased during the ASL period (indicated by horizontal bars), then recovered during the control period. In the artery-containing ROI (white square in the inset image), the signal decrease was more rapid and greater as compared with the somatosensory cortex (filled vs. open red circles). Fitting of the experimental data with Eq. 1 was quite good for the somatosensory cortex (open red and blue circles for N = 40 and N = 80, respectively), but not for areas with a large arterial contribution (filled red circles), indicating that the single-compartment ASL model is reasonable for ROI with a minimal arterial contribution, such as the cortex. To determine the effect of Turbo-DASL imaging parameters on CBF and TT quantification, CBF and TT_a determined from the somatosensory ROI were compared across four different conditions (TR = 100 ms and 200 ms, with N = 40 or 80). Turbo-DASL data with TR = 100 ms and N = 40 and 80 yielded CBF of 1.20 and 1.30 ml/g/min and TT_a of 286 and 310 ms, respectively. When TR was increased to 200 ms, the measured CBF values were 1.34 and 1.51 ml/g/min and the TT_a values were 295 and 302 ms, for N = 40 and 80, respectively. Although TT_a was insensitive to the Turbo-DASL parameters, the measured CBF values slightly increased with TR and N. Our data indicates that the duration of control and labeling periods affected the fitting convergence. When the ASL period is longer (e.g., increased N and/or TR),

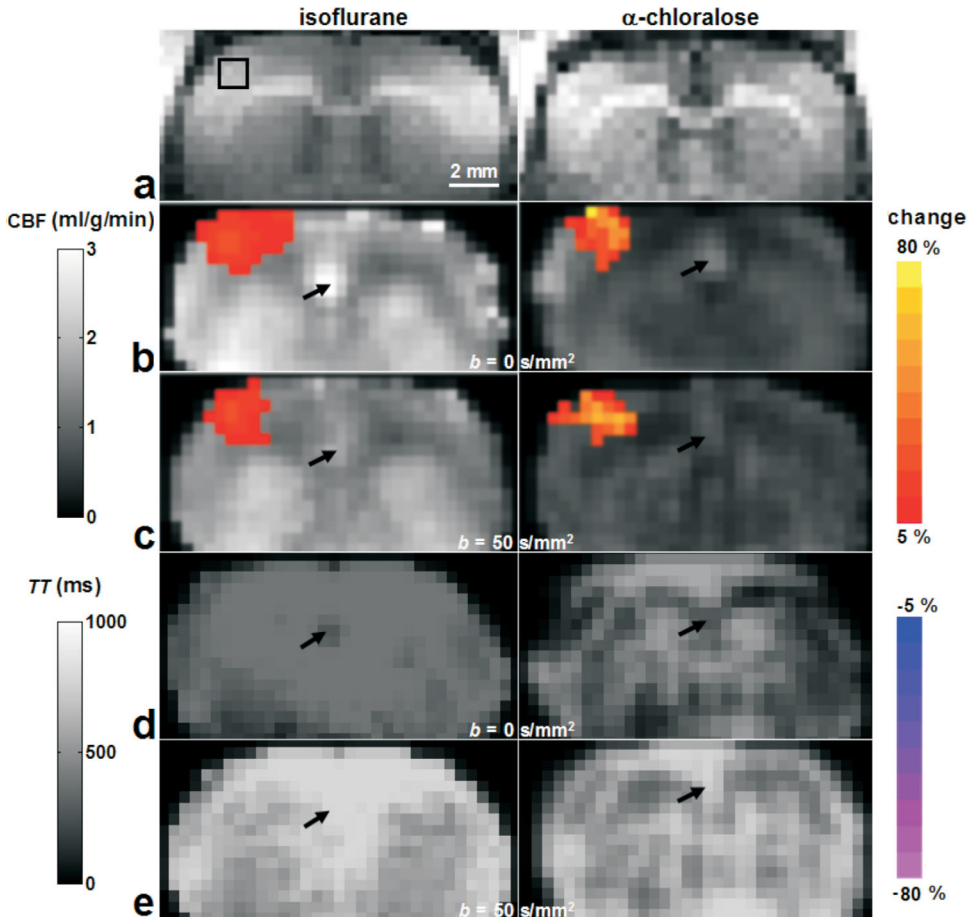

FIG. 3. Baseline and functional Turbo-DASL results from two rats, anesthetized with isoflurane (left) and α-chloralose (right). Gray-scale background maps (except the anatomical T_1-weighted image (**a**)) were quantitative CBF values obtained without and with diffusion gradients ((**b**) and (**c**), respectively) and TT values without and with diffusion gradients ((**d**) and (**e**), respectively). Color maps overlaid on baseline images were percent changes of active pixels responding to forepaw stimulation. On the anatomical T_1-weighted images (a), the black box indicates the 3 × 3 pixel ROI in the contralateral area, which will be used for further data analysis. Arrows indicate one large arterial vessel region, where the diffusion gradient of 50 s/mm^2 changed the computed baseline CBF and TT.

the steady-state condition is better satisfied and the calculated CBF is likely to be more accurate.

Baseline CBF and TT maps were calculated from Turbo-DASL data with TE = 100 ms and $N = 40$ for isoflurane- and α-chloralose-anesthetized animals (Fig. 3 gray-scale background images). CBF values determined without diffusion gradients were 20–30% higher than those with flow-crushing gradients (Fig. 3b vs. c background), and CBF values in rats under α-chloralose anesthesia (right column) were about 50–60% of that measured in rats under isoflurane anesthesia (left column). Baseline TT values obtained without and with diffusion gradients were 300–400 ms (Fig. 3d) and 500–700 ms (Fig. 3e), respectively. The diffusion gradients had a major impact on pixels that contained signal from large vessels (indicated by black arrows) by reducing computed CBF and increasing calculated TT to values of neighbor tissue pixels.

Baseline CBF, TT_a, TT_c, and CBV_a determined from the contralateral somatosensory ROI (black square in Fig. 3a) were tabulated in Table 1. Note that CBF was determined from data with a diffusion gradient to minimize arterial blood contributions. Baseline CBF and CBV_a in rats under α-chloralose anesthesia were 50–60% of those in rats anesthetized with isoflurane ($P < 0.05$). Baseline TT_a and TT_c values were not statistically different for isoflurane vs. α-chloralose anesthesia.

Functional Responses in Isoflurane- and α-Chloralose-Anesthetized Animals

During forepaw stimulation, localized CBF changes were observed in the contralateral somatosensory cortex of animals under both anesthetics, while no significant changes in TT_c and TT_a were detected (Fig. 3 color maps). Time courses of the contralateral somatosensory ROI were obtained from the same animals shown in Fig. 3 and then plotted in Fig. 4. Time courses of CBF and TT were similar for with (dashed lines) vs. without diffusion gradients (solid lines), although there were different baseline values. Under α-chloralose anesthesia (Fig. 4c), functional changes in CBF were much larger and more constant than those under isoflurane (Fig. 4a). However, no significant changes in TT were observed, except during stimulus on-and-off transition periods. As dynamic changes in CBF and TT during the transition periods

Table 1
Turbo-DASL Results of Isoflurane-Anesthetized ($n = 7$) and α-Chloralose-Anesthetized ($n = 5$) Rats in Baseline and Somatosensory Stimulation Conditions

Anesthetic	Absolute values in baseline condition		Absolute values in stimulation (functional percentage changes)	
	Isoflurane	α-Chloralose	Isoflurane	α-Chloralose
CBF (ml/g/min)[a]	1.05 ± 0.25	0.66 ± 0.14*	1.21 ± 0.28† (15 ± 3%)	1.06 ± 0.23† (60 ± 7%)
TT_a (ms)	381 ± 86	396 ± 48	376 ± 86 (−1 ± 3%)	383 ± 44 (−3 ± 3%)
TT_c (ms)	636 ± 83	714 ± 37	627 ± 92 (−2 ± 3%)	698 ± 40 (−2 ± 2%)
CBV_a (ml/100 g)	0.59 ± 0.26	0.30 ± 0.14*	0.69 ± 0.29† (19 ± 9%)	0.44 ± 0.19† (46 ± 17%)

All values were obtained from contralateral somatosensory cortical ROIs with 3 × 3 pixels (mean ± SD). TT_a: arterial blood transit time from the carotid arteries to cortical arteries; TT_c: arterial blood transit time from carotid arteries to capillaries; CBV_a: cerebral arterial blood volume.
[a]CBF was measured with diffusion gradients ($b = 50$ s/mm^2).
*Significantly different from values in the baseline condition under isoflurane anesthesia ($P < 0.05$, independent two sample t-test).
†Significantly different from values in the baseline condition under the same anesthesia ($P < 0.05$, paired two-tailed t-test).

between baseline and stimulation conditions (e.g., 0–4 s) introduce errors in CBF and TT quantification from Turbo-DASL data, transition data points were excluded for quantitative ROI analysis.

Quantitative CBF, TT_a, TT_c, and CBV_a determined from the contralateral somatosensory ROI (black square in Fig. 3a) during stimulation were tabulated in Table 1. Note that CBF was calculated from data with diffusion gradients to minimize arterial blood contributions, even though relative changes in blood flow measured without and with diffusion gradients were similar (data not shown). Significant increases in CBF and CBV_a were detected under isoflurane and α-chloralose anesthesia ($P < 0.05$). However, TT_a and TT_c did not change significantly during stimulation under both anesthetic conditions ($P > 0.05$).

Relationship Between CBF, TT, and Arterial CBV

Data from each subject during baseline and stimulation periods were plotted in Fig. 5, and the change in TTs and CBV_a were plotted against the corresponding change in CBF in Fig. 6. As shown in Fig. 5a–c, shorter TT_a, TT_c, and blood TT from arteries to capillaries (i.e., $TT_c - TT_a$) were accompanied by higher CBF values during baseline and stimulation conditions under both anesthetics, albeit

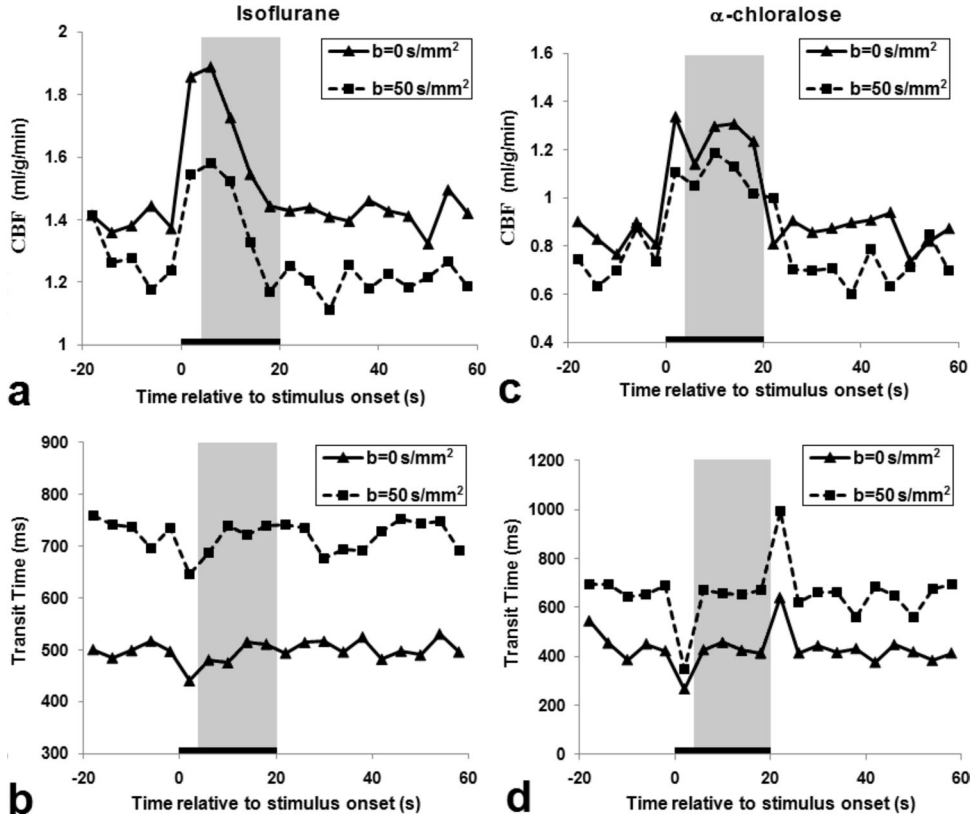

FIG. 4. Time courses of CBF and TT in the contralateral somatosensory ROI from two rats shown in Fig. 3 under isoflurane ((**a**), (**b**)) and α-chloralose ((**c**), (**d**)) anesthesia, measured without ($b = 0$ s/mm^2) and with diffusion gradients ($b = 50$ s/mm^2). The black bar indicates the 20-s stimulus period, while the gray-highlighted region indicates the stimulation time period (i.e., 4–20 s) used for further data analysis in Figs. 5 and 6 and Table 1.

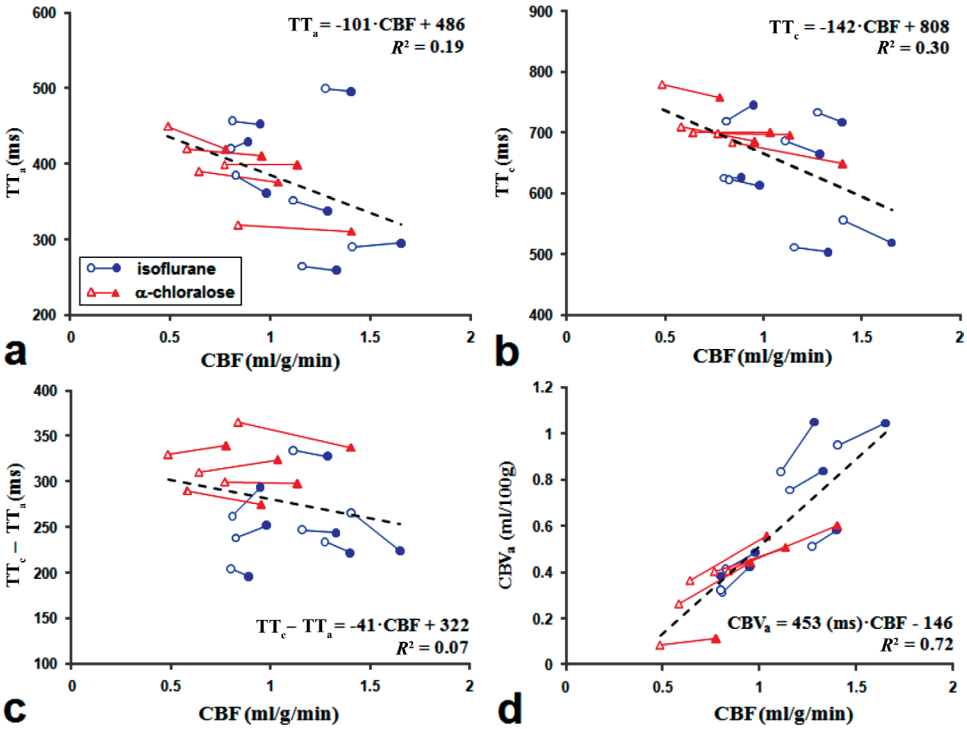

FIG. 5. Interanimal relationships between physiological parameters obtained from Turbo-DASL data. CBF values measured with diffusion gradients (b = 50 s/mm^2) at baseline (open symbols) and stimulation (filled symbols) in each animal (connected line) were plotted against corresponding TT_a (**a**), TT_c (**b**), TT_c – TT_a (**c**), and CBV_a (**d**). Blue circles with blue lines and red triangles with red lines represent data measured from animals anesthetized with isoflurane and α-chloralose, respectively. The dash lines show a linear fit for all points on each plot. When CBV_a is linearly correlated with CBF (d) with zero intercept, CBV_a (ml/100 g) = 320 (ms)·CBF (ml/100 g/min). [Color figure can be viewed in the online issue, which is available at wileyonlinelibrary.com.]

weakly correlated. Similarly, functional change of (TT_c – TT_a) was poorly or not correlated with CBF change (Fig. 6a and b). As expected, the absolute CBF value was highly correlated with the absolute CBV_a ($R^2 > 0.7$; Fig. 5d), and functional CBF change was highly correlated to functional CBV_a response (Fig. 6c and d).

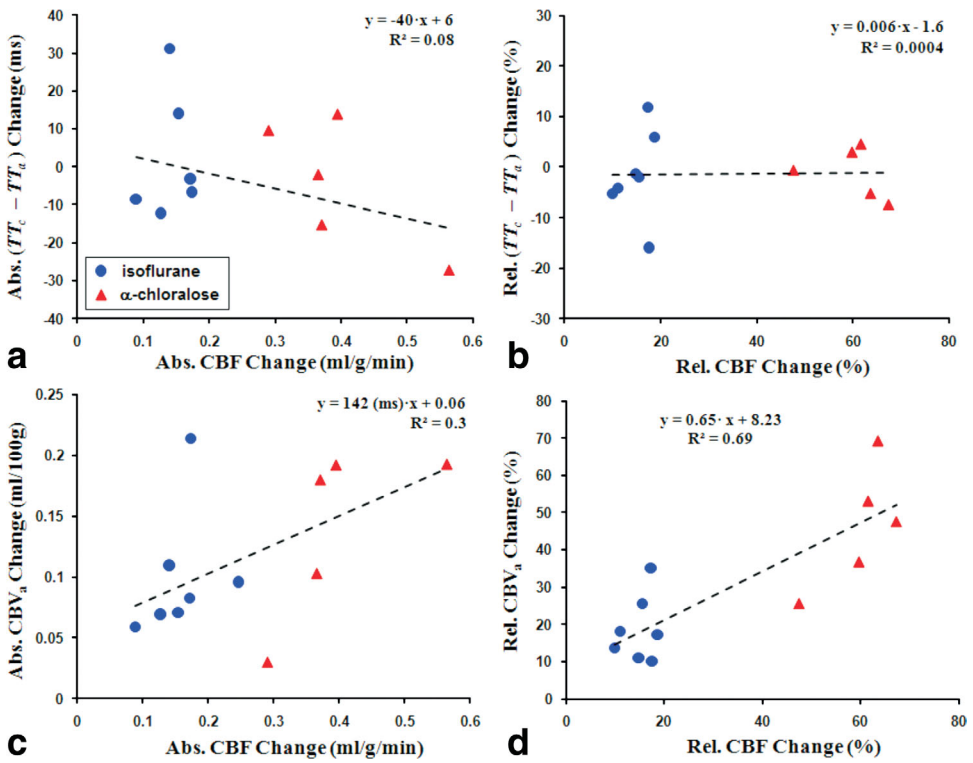

FIG. 6. Absolute (Abs.) and relative (Rel.) functional changes in CBF vs. TT_c – TT_a ((**a**) and (**b**)), and CBF vs. CBV_a ((**c**) and (**d**)). CBF values were measured with diffusion gradients (b = 50 s/mm^2). Blue circles and red triangles represent data obtained from isoflurane and α-chloralose anesthetized rats, respectively. The dash lines show a linear fit for all points on each plot. When functional CBF vs. CBV_a relationship was obtained with zero intercept, ΔCBV_a (ml/100 g) = 244 (ms)·ΔCBF (ml/100 g/min) and ΔCBV_a (%) = 0.82·ΔCBF (%). [Color figure can be viewed in the online issue, which is available at wileyonlinelibrary.com.]

DISCUSSION

Technical Aspects of Turbo-DASL

Using the Turbo-DASL method, CBF and TT were obtained with high temporal resolution, facilitating hemodynamic measurements. This approach relies on several assumptions: (i) the one-compartment ASL model is appropriate, (ii) no dynamic changes of CBF and TT occur during one Turbo-DASL cycle, and (iii) the arterial blood signals are not affected by repeated excitations. As mentioned in the Results section, fitting Turbo-DASL data with Eq. 1 is also dependent on ASL and control durations. Because of the use of a 2-s ASL duration for fMRI studies, our calculation yields a slightly underestimated CBF.

In our application, we adopted the single-compartment model. When tissue-dominant pixels are chosen, the single-compartment model fits the data well, as seen in the cortex (see Fig. 2). However, when arterial blood signals contribute significantly (as shown in the artery ROI in Fig. 2 and indicated by arrows in Fig. 3), the single-compartment model is not appropriate; short TT_a and high CBF values were observed when fitting data with Eq. 1. For this data, a two-compartment (blood and tissue) ASL model can be used to determine CBF, TT_a and TT_c, but the accuracy of these parameters is poor due to limited number of data points.

Dynamic changes in physiological parameters during one Turbo-DASL cycle will generate errors in the calculated CBF and TT because the ASL model assumes a steady-state condition, as seen in Fig. 4. Even if CBF and TT do not change during a 4-s period, dynamic change in blood oxygen level dependent signals (in this case $M(0) \neq M_{eq}$) will induce errors in CBF and TT estimations. In our computer stimulations with baseline CBF and TT values shown in Table 1, the calculated TT would decrease up to 7% if the blood oxygen level dependent signal linearly increased to 1% during 4 s without CBF and TT changes. When large, rapid, hemodynamic changes occurred in the transition periods between baseline and stimulation periods, large erroneous changes in TT were observed (especially in Fig. 4d). This error can be reduced by shortening each Turbo-DASL cycle; however, the sensitivity of ASL-induced signals is reduced, leading to larger errors in fitting. To take into account these dynamic changes, a more complex model needs to be established with varying TT and other hemodynamic changes with different onset times; however, the limited number of data points available for fitting precludes the use of a more complex model. Thus, in our study these transition periods were excluded from the calculations.

Quantification of CBF and CBV_a values is closely dependent on accuracy of ASL efficiency. The assumption of no arterial blood signal saturations by repeated excitations is not likely valid. Arterial blood travels within arterial vasculature during $TT_c - TT_a$ (e.g., ~300 ms) before it enters into the capillaries and will experience repeated RF excitations at every TR of 100 ms, consequently reducing the spin labeling efficiency. Although the exact saturation level of arterial blood signals is related to RF flip angle, TR and $TT_c - TT_a$, it is pretty clear that our spin labeling efficiency value was overestimated, resulting in an underestimation of CBF and CBV_a values. However, the relative changes in CBF and CBV_a are valid because the errors canceled each other out. Also, the determination of TT is independent of the accuracy of the spin labeling efficiency, although TT_a (381 ms) in the somatosensory cortex determined under isoflurane anesthesia is slightly longer than that previously obtained under halothane anesthesia (223 ms) (7) or isoflurane anesthesia (260 ms) (16).

Baseline Physiological Parameters Under Different Anesthetics

The CBF values obtained with Turbo-DASL, 1.05 ml/g/min in rats under isoflurane and 0.66 ml/g/min in rats under α-chloralose, are slightly lower than or similar to CBF values previously obtained, 1.5 ml/g/min under isoflurane (20,31) and 0.6–0.91 ml/g/min under α-chloralose (30,32–34). The CBV_a value under isoflurane obtained from Turbo-DASL (0.59 ml/100 g) is less than the reported value with the same animal model, 0.8–1.1 ml/100 g (20,35). If the same error between the CBV_a values under isoflurane obtained from Turbo-DASL and the previous reports (20,35) also occurred under α-chloralose, the expected CBV_a is 0.41–0.56 ml/100 g under α-chloralose.

As expected, rats anesthetized with the two different anesthetics exhibited different baseline CBF and CBV_a values. CBF and CBV_a with α-chloralose were ~60% and ~50% of that found with isoflurane, respectively. However, the measured TTs were similar for both anesthetic conditions. When all animals were compared together, higher absolute CBF values were associated with higher CBV_a (Fig. 5d) and lower TT (Fig. 5b). These results agree with previous studies during global CO_2 modulation where CBF is positively correlated with CBV_a (20,32), and CBF is inversely correlated with TT (15,16). This indicates that higher CBF accompanies a higher blood velocity and a shorter blood TT from the carotid arteries to cortical vessels.

The difference between TT_c and TT_a is the time that blood has spent in the cortical arterial vasculature, which is referred to as the mean TT (MTT) of blood throughout the arterial vasculature. This can be also determined by the central volume principle MTT = CBV_a/CBF. The baseline MTT of arterial vasculature calculated from CBV_a and CBF is about 337 ms for rats under isoflurane and about 272 ms rats under α-chloralose, which is similar to 255 ms and 318 ms ($TT_c - TT_a$ in Table 1), respectively. Note that the definition of conventional MTT differs from MR-measured TT_a or TT_c.

Physiological Changes Induced by Forepaw Stimulation Under Two Different Anesthetics

During neural stimulation, CBF and CBV_a increased 15% and 19% for rats under isoflurane anesthesia and increased 60% and 46% for rats under α-chloralose anesthesia, respectively. Our observation that an increase in CBF is mostly due to an increase in CBV_a (see Figs. 5d and 6c and d) agrees well with our laboratory's previous CBF and CBV_a measurements using the same animal model under isoflurane anesthesia (20,36). Although

changes in CBF and CBV_a depend on different stimulus parameters and different animal physiological conditions, our findings with these anesthetics show similar trends to previous measurements using isoflurane (28) and α-chloralose (21). Under isoflurane, CBF was not maintained during the 20-s stimulation period unlike under α-chloralose (Fig. 4a vs. c). This is not due to methodological problems but due to genuine vascular responses. Neural activities and CBF responses quickly decrease during the stimulation period due to neural adaptation effects (28). The dynamic functional CBF change during the stimulation period is closely dependent on the physiological condition of the animal and isoflurane level (37).

During stimulation, TT_a and TT_c slightly decreased in most animals (Fig. 5a and b), albeit the decrease was statistically insignificant (Table 1), and a higher CBF increase appeared to have a larger MTT change (Fig. 6a). In several previous studies in rodents, a CO_2 challenge resulted in a significant decrease in TT_a while CBF increased (15,16,38). This apparent difference can be due to different vascular regulation mechanisms of local neural activity vs. a global CO_2 challenge and due to the different stimulation periods. In our forepaw stimulation studies, the 20-s stimulation period led mostly to only dilation of the arterial vessels (36,39) because venous vessels dilate slowly and passively. A long stimulation period is often used for CO_2 studies; therefore, both arterial and venous vessels dilate (32), which reduces the venous resistance and consequently increases the upstream arterial blood velocity.

Our functional TT_a and TT_c data differ from human studies in which significant TT decreases were detected during stimulation (8,10,12,14,19). In visual cortex, Francis et al. (8) reported that TT_a and TT_c decreased 14–20%, while CBF increased 86%; Ho et al. (12) reported that TT_c decreased 15–25% from 780 ms while CBF increased 42–66%. In motor cortex, Yang et al. (19) reported that TT_a decreased 17% from 650 ms while CBF increased 80%. With a motor and visual task, Gonzalez-At et al. (14) observed a significant decrease in TT_a, about 150 ms from 850 ms, while CBF increased 30% during stimulation. As baseline TT is much larger in the human brain than in small animals, a change in TT is more easily detectable in humans relative to small animals. Potentially important confounding effects are stimulation duration and type, which will determine arterial vs. venous CBV change and consequently arterial blood velocity change (36).

There are numerous non-MR measurements of blood velocity and/or arterial-to-venous TT of blood during stimulation. Capillary blood velocity changes have been measured by laser Doppler (40) and by two-photon laser scanning microscopy (41,42). There are two common observations in literature: increasing capillary velocity (41–43) and shortening arterial-to-venous MTT during stimulation (44). During a 20-s somatosensory stimulation, arterial vessels dilate significantly (20,36,39) with little or small arterial blood velocity increase, while capillaries and venous vessels do not dilate much (39), consequently increasing blood velocity. Thus, capillary blood velocity increases, and arterial-to-venous MTT is shortened during stimulation. These non-MR findings do not disagree with our Turbo-DASL data.

CONCLUSION

In summary, we have developed a novel Turbo-DASL technique to rapidly measure arterial blood TT and blood flow and applied it without and with diffusion gradients to anesthetized rats. Baseline CBF and CBV_a were much less in rats under α-chloralose than under isoflurane, while TT_a and TT_c were similar for both anesthetic conditions. During forepaw stimulation, relative CBF and CBV_a changes in the somatosensory cortex were higher for rats under α-chloralose than under isoflurane. However, TT_a and TT_c were not significantly changed. These results indicate that there is minimal arterial blood velocity change during somatosensory stimulation and support the hypothesis that arterial dilation plays an important role in functional CBF increase.

ACKNOWLEDGMENTS

The authors thank Kristy Hendrich for maintaining the MR system, and Tae Kim for helpful discussions.

REFERENCES

1. Williams DS, Detre JA, Leigh JS, Koretsky AP. Magnetic resonance imaging of perfusion using spin inversion of arterial water. Proc Natl Acad Sci USA 1992;89:212–216.
2. Kim SG. Quantification of relative cerebral blood flow change by flow-sensitive alternating inversion recovery (FAIR) technique: application to functional mapping. Magn Reson Med 1995;34:293–301.
3. Edelman RR, Chen Q. EPISTAR MRI: multislice mapping of cerebral blood flow. Magn Reson Med 1998;40:800–805.
4. Wong EC, Buxton RB, Frank LR. Quantitative imaging of perfusion using a single subtraction (QUIPSS and QUIPSS II). Magn Reson Med 1998;39:702–708.
5. Alsop DC, Detre JA. Reduced transit-time sensitivity in noninvasive magnetic resonance imaging of human cerebral blood flow. J Cereb Blood Flow Metab 1996;16:1236–1249.
6. Chalela JA, Alsop DC, Gonzalez-Atavales JB, Maldjian JA, Kasner SE, Detre JA. Magnetic resonance perfusion imaging in acute ischemic stroke using continuous arterial spin labeling. Stroke 2000;31:680–687.
7. Thomas DL, Lythgoe MF, van der Weerd L, Ordidge RJ, Gadian DG. Regional variation of cerebral blood flow and arterial transit time in the normal and hypoperfused rat brain measured using continuous arterial spin labeling MRI. J Cereb Blood Flow Metab 2006;26:274–282.
8. Francis ST, Bowtell R, Gowland PA. Modeling and optimization of look-locker spin labeling for measuring perfusion and transit time changes in activation studies taking into account arterial blood volume. Magn Reson Med 2008;59:316–325.
9. Günther M, Bock M, Schad L. Arterial spin labeling in combination with a look-locker sampling strategy: inflow turbo-sampling EPI-FAIR (ITS-FAIR). Magn Reson Med 2001;46:974–984.
10. Hendrikse J, Lu H, van der GJ, van Zijl PC, Golay X. Measurements of cerebral perfusion and arterial hemodynamics during visual stimulation using TURBO-TILT. Magn Reson Med 2003;50:429–433.
11. Petersen ET, Lim T, Golay X. Model-free arterial spin labeling quantification approach for perfusion MRI. Magn Reson Med 2006;55:219–232.
12. Ho YC, Petersen ET, Golay X. Measuring arterial and tissue responses to functional challenges using arterial spin labeling. Neuroimage 2010;49:478–487.
13. Wang J, Alsop DC, Song HK, Maldjian JA, Tang K, Salvucci AE, Detre JA. Arterial transit time imaging with flow encoding arterial spin tagging (FEAST). Magn Reson Med 2003;50:599–607.
14. Gonzalez-At JB, Alsop DC, Detre JA. Cerebral perfusion and arterial transit time changes during task activation determined with continuous arterial spin labeling. Magn Reson Med 2000;43:739–746.

15. Barbier EL, Silva AC, Kim HJ, Williams DS, Koretsky AP. Perfusion analysis using dynamic arterial spin labeling (DASL). Magn Reson Med 1999;41:299–308.
16. Barbier EL, Silva AC, Kim SG, Koretsky AP. Perfusion imaging using dynamic arterial spin labeling (DASL). Magn Reson Med 2001;45: 1021–1029.
17. Faraci FM, Heistad DD. Regulation of the cerebral circulation: role of endothelium and potassium channels. Physiol Rev 1998;78:53–97.
18. Hamel E. Perivascular nerves and the regulation of cerebrovascular tone. J Appl Physiol 2006;100:1059–1064.
19. Yang Y, Engelien W, Xu S, Gu H, Silbersweig DA, Stern E. Transit time, trailing time, and cerebral blood flow during brain activation: measurement using multislice, pulsed spin-labeling perfusion imaging. Magn Reson Med 2000;44:680–685.
20. Kim T, Hendrich KS, Masamoto K, Kim SG. Arterial versus total blood volume changes during neural activity-induced cerebral blood flow change: implication for BOLD fMRI. J Cereb Blood Flow 2007; 27:1235–1247.
21. Silva AC, Lee SP, Yang G, Iadecola C, Kim SG. Simultaneous blood oxygenation level-dependent and cerebral blood flow functional magnetic resonance imaging during forepaw stimulation in the rat. J Cereb Blood Flow Metab 1999;19:871–879.
22. Kim T, Kim SG. Quantification of cerebral arterial blood volume using arterial spin labeling with intravoxel incoherent motion-sensitive gradients. Magn Reson Med 2006;55:1147–1157.
23. Buxton RB, Frank LR, Wong EC, Siewert B, Warach S, Edelman RR. A general kinetic model for quantitative perfusion imaging with arterial spin labeling. Magn Reson Med 1998;40:383–396.
24. Paxinos G, Watson C. The rat brain in stereotaxic coordinates. San Diego: Academic Press; 1986.
25. Meng Y, Lei H. An efficient gridding reconstruction method for multishot non-Cartesian imaging with correction of off-resonance artifacts. Magn Reson Med 2010;63:1691–1697.
26. Insko EK, Bolinger L. Mapping of the radiofrequency field. J Magn Reson 1993;103:82–85.
27. Masamoto K, Kim T, Fukuda M, Wang P, Kim SG. Relationship between neural, vascular and BOLD signals in isoflurane-anesthetized rat somatosensory cortex. Cereb Cortex 2007;17:942–950.
28. Kim T, Masamoto K, Fukuda M, Vazquez A, Kim SG. Frequency-dependent neural activity, CBF, and BOLD fMRI to somatosensory stimuli in isoflurane-anesthetized rats. Neuroimage 2010;52:224–233.
29. Zhang W, Williams DS and Koretsky AP. Measurement of rat brain perfusion by NMR using spin labeling of arterial water: in vivo determination of the degree of spin labeling. Magn Reson Med 1993;29:416–421.
30. Tsekos NV, Zhang F, Merkle H, Nagayama M, Iadecola C, Kim S-G. Quantitative measurements of cerebral blood flow in rats using the FAIR technique: correlation with previous iodoantipyrine autoradiographic studies. Magn Reson Med 1998;39:564–573.
31. Maekawa T, Tommasino C, Shapiro HM, Keifer-Goodman J, Kohlenberger RW. Local cerebral blood flow and glucose utilization during isoflurane anesthesia in the rat. Anesthesiology 1986;65:144–151.
32. Lee SP, Duong TQ, Yang G, Iadecola C, Kim SG. Relative changes of cerebral arterial and venous blood volumes during increased cerebral blood flow: implications for BOLD fMRI. Magn Reson Med 2001;45: 791–800.
33. Duong TQ, Kim SG. In vivo MR measurements of regional arterial and venous blood volume fractions in intact rat brain. Magn Reson Med 2000;43:393–402.
34. Ueki M, Linn F, Hossmann KA. Functional activation of cerebral blood flow and metabolism before and after global ischemia of rat brain. J Cereb Blood Flow Metab 1988;8:486–494.
35. Kim T, Kim SG. Quantification of cerebral arterial blood volume and cerebral blood flow using MRI with modulation of tissue and vessel (MOTIVE) signals. Magn Reson Med 2005;54:333–342.
36. Kim T, Kim SG. Temporal dynamics and spatial specificity of arterial and venous blood volume changes during visual stimulation: implication for BOLD quantification. J Cereb Blood Flow Metab 2011;31: 1211–1222.
37. Masamoto K, Fukuda M, Vazquez A, Kim SG. Dose-dependent effect of isoflurane on neurovascular coupling in rat cerebral cortex. Eur J Neurosci 2009;30:242–250.
38. Wegener S, Wu WC, Perthen JE, Wong EC. Quantification of rodent cerebral blood flow (CBF) in normal and high flow states using pulsed arterial spin labeling magnetic resonance imaging. J Magn Reson Imaging 2007;26:855–862.
39. Drew PJ, Shih AY, Kleinfeld D. Fluctuating and sensory-induced vasodynamics in rodent cortex extend arteriole capacity. Proc Natl Acad Sci USA 2011;108:8473–8478.
40. Barfod C, Akgören N, Fabricius M, Dirnagl U, Lauritzen M. Laser-Doppler measurements of concentration and velocity of moving blood cells in rat cerebral circulation. Acta Physiol Scand 1997;160: 123–132.
41. Kleinfeld D, Mitra PP, Helmchen F, Denk W. Fluctuations and stimulus-induced changes in blood flow observed in individual capillaries in layers 2 through 4 of rat neocortex. Proc Natl Acad Sci USA 1998; 95:15741–15746.
42. Chaigneau E, Oheim M, Audinat E, Charpak S. Two-photon imaging of capillary blood flow in olfactory bulb glomeruli. Proc Natl Acad Sci USA 2003;100:13081–13086.
43. Detre JA, Ances BM, Takahashi K, Greenberg JH. Signal averaged laser Doppler measurements of activation–flow coupling in the rat forepaw somatosensory cortex. Brain Res 1998;796:91–98.
44. Woolsey TA, Rovainen CM, Cox SB, Henegar MH, Liang GE, Liu D, Moskalenko YE, Sui J, Wei L. Neuronal units linked to microvascular modules in cerebral cortex: response elements for imaging the brain. Cereb Cortex 1996;6:647–460.